

The value of  $\bar{U}(r_{\min})$  is, therefore, very sensitive to the value chosen for  $q_{\max}$ . For the Bloch-Nordsieck method to be applicable, we may suppose  $q_{\max} < (1/20) \times \text{Debye cutoff}$ , i.e.,  $q_{\max} \leq 5 \times 10^6$ . Then  $r_{\min} = 2 \times 10^{-7}$ . This gives

$$\bar{U}(r_{\min}) \approx 10^{-2} \text{ ev,}$$

which is the same as that given by Fröhlich using the second-order perturbation theory. It should be clearly understood that the above choice of  $q_{\max}$  is entirely arbitrary and there is nothing in the B-N method to guide us in this respect except that the momenta of the phonons have to be much less than those of the electrons with which they interact.

## Piezoresistance Effect in Germanium and Silicon

CHARLES S. SMITH

*Bell Telephone Laboratories, Murray Hill, New Jersey*

(Received December 30, 1953)

Uniaxial tension causes a change of resistivity in silicon and germanium of both  $n$  and  $p$  types. The complete tensor piezoresistance has been determined experimentally for these materials and expressed in terms of the pressure coefficient of resistivity and two simple shear coefficients. One of the shear coefficients for each of the materials is exceptionally large and cannot be explained in terms of previously known mechanisms. A possible microscopic mechanism proposed by C. Herring which could account for one large shear constant is discussed. This so called electron transfer effect arises in the structure of the energy bands of these semiconductors, and piezoresistance may therefore give important direct experimental information about this structure.

### INTRODUCTION

THE effect of pure hydrostatic pressure on resistance has been extensively studied, notably by Bridgman, who also made the first piezoresistance measurements<sup>1</sup> known to us on several polycrystalline metals. Bridgman has also outlined the formal nature of the piezoresistance effect in single crystals<sup>2</sup> and applied this analysis to the measurements of Allen<sup>3</sup> on bismuth. Cookson<sup>4</sup> later corrected the original outline by Bridgman. Allen has reported single crystal tension coefficients in addition for tin,<sup>5</sup> antimony,<sup>6</sup> and zinc and cadmium.<sup>7</sup> The present observations<sup>8</sup> for germanium and silicon are apparently the first for cubic crystals and the first giving the complete tensor.

The change in resistance caused by stress induced dimensional changes is small and may be corrected for, allowing any remaining effect to be expressed as a change in resistivity  $\rho$ . The resistivity may be stress dependent through either the mobility or the number of the charge carriers. The effect of stress on the mobility of the charge carriers has been observed for many materials. For example, values of  $d \ln \rho / d \ln v$  running

from two to six are reported for pressure experiments,<sup>9</sup> these values agree fairly well for a number of metals with a simple calculation<sup>9</sup> of the change of mobility produced by the change in the amplitude of thermal vibrations with volume  $v$ ,

$$(d \ln \rho / d \ln v) = (2\alpha v_0 / \chi_0 C_v), \quad (1)$$

where  $\alpha$  is the thermal expansion coefficient,  $\chi$  the compressibility, and  $C_v$  the specific heat. For silicon and germanium the calculated values of this quantity are 1.4 and 1.7.

In semiconductors the stress may be expected to change the number of charge carriers. The stress  $X$  causes a volume change  $\delta v$  which in turn causes a change  $\delta E_g$  in the energy gap between the valence and conduction bands. The number of carriers and hence the resistivity therefore change. For germanium at 300°K  $\delta E_g = -4.0 d \ln v$  (electron volts),<sup>10</sup> and for intrinsic germanium this means that  $d \ln \rho_i / d \ln v = -77$ . This volume-energy gap effect can be shown to be roughly proportional to  $(\rho / \rho_i)^2$ ; the observations reported below were carried out at values of  $(\rho / \rho_i)^2$  where the energy gap effect is detectable but small.

The piezoresistance results for germanium and silicon which are reported here have been expressed in terms of the pressure coefficient of resistivity and two simple shear coefficients. One of the shear coefficients for each of the materials is exceptionally large and cannot be

<sup>1</sup> P. W. Bridgman, Proc. Am. Acad. Arts Sci. **60**, 423 (1925).

<sup>2</sup> P. W. Bridgman, Phys. Rev. **42**, 858 (1932).

<sup>3</sup> Mildred Allen, Phys. Rev. **42**, 848 (1932).

<sup>4</sup> J. W. Cookson, Phys. Rev. **47**, 194 (1935).

<sup>5</sup> Mildred Allen, Phys. Rev. **52**, 1246 (1937).

<sup>6</sup> Mildred Allen, Phys. Rev. **43**, 569 (1933).

<sup>7</sup> Mildred Allen, Phys. Rev. **49**, 248 (1936).

<sup>8</sup> The large tension effects were noticed in these laboratories by J. R. Haynes. The stress sensitive drift mobility observed by Lawrence in  $n$  germanium is probably the same effect. R. Lawrence, Phys. Rev. **89**, 1295 (1953).

<sup>9</sup> N. F. Mott and H. Jones, *The Theory of the Properties of Metals and Alloys* (Oxford University Press, London, 1936), p. 271.

<sup>10</sup> J. H. Taylor, Phys. Rev. **80**, 919 (1950).

explained in terms of these previously known mechanisms. The mobility mechanism appears to be too small to account for the magnitude of the large shear coefficient, and the energy gap effect gives zero contribution to both shear coefficients. Thus the explanation of the salient feature of the present work must be sought in an essentially new mechanism.

### EXPERIMENTAL

As shown in the Appendix it is necessary to make three experimental measurements of at least two types in order to determine the complete piezoresistance in germanium and silicon. The essential features of the arrangements which have been used are shown in Fig. 1. Uniaxial tensile stress  $X$  was applied to single crystal rods by hanging a weight on a string, and the  $IR$  drop was measured. The two crystal orientations shown in the figure were used in combination with the two electrode configurations shown, yielding the necessary three measurements of two types. The extra measurement was made for a few specimens as an internal check.

### Procedure

The  $IR$  drop across the potential electrodes was read by a type-K potentiometer. The stress induced difference potential  $\delta V$  was indicated directly in microvolts on the output meter of a Type-9835A Leeds and Northrup dc amplifier.

The observational procedure was to load the specimen, balance the potentiometer at a convenient meter reading, lift the weight and replace it, observing the throw of the output meter  $\delta V$ , and then to repeat the process for the next load. The potential change  $\delta V$  was found to reverse with the sign of the stress, to show no detectable hysteresis, and to be linear with load in the range employed.

The fast response of the indicating instrument made it possible to make the observations in spite of small drifts caused by ambient temperature changes. The electrical observations were all made at *constant current* supplied from a 300-volt, 300 000-ohm source. The potentials  $V$  ranged all the way from a few millivolts to a few volts for the different electrode arrangements and resistivity values studied. Loads ranging from 0.1 to 1 kg were applied, corresponding to stress levels from  $10^7$  to  $10^8$  dyne  $\text{cm}^{-2}$ . In the constant current case  $\delta V/V = \delta R/R$ ; values of this quantity ran from  $10^{-5}$  to  $10^{-3}$  for different specimens.

### Materials and Specimen Preparation

The starting materials were single crystals of As-doped  $n$ -type germanium and Ga-doped  $p$ -Ge and silicon crystals which were grown  $n$  or  $p$  from selected raw material. The crystals were oriented on an x-ray goniometer. The individual specimens A, B, C, D (Fig. 1), of a given nominal resistivity value were cut

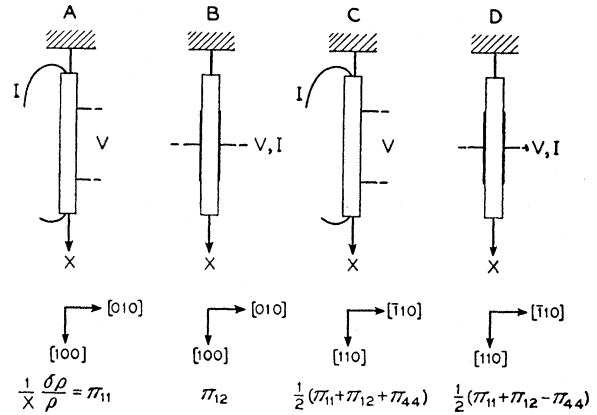


FIG. 1. Schematic diagram showing the stress system, the crystallographic orientations and the electrode structures which have been used. Arrangements A and C are designated as longitudinal in the text; B and D are called transverse.

from adjacent slices to hold the resistivity variation within the group to 10 percent. The specimen ends were waxed into small grips with sealing wax in the transverse cases (B, D), or rhodium plated and soldered in the longitudinal cases (A, C). The grips were aligned manually with only small difficulties from misalignment as noted below. The long transverse electrodes were rhodium and copper plated.

### Corrections

The directly observed quantity in the present experiments is  $(1/X)(\delta R/R)$ , which must be corrected for dimensional changes to yield  $(1/X)(\delta \rho/\rho)$  by adding for the several cases as follows:

$$\begin{aligned} \text{(A), } & -(S_{11} - 2S_{12}); & \text{(C), } & -(\frac{1}{2}S_{44} - S_{12}); \\ \text{(B), } & +S_{11}; & \text{(D), } & +(\frac{1}{2}S_{44} + S_{12}). \end{aligned}$$

The elastic compliances  $S_{ij}$  are well known for silicon and germanium.<sup>11</sup>

The transverse measurements are then subject to another correction which arises because the current lines are not straight at the ends of the electrodes. Such a correction would not be necessary if the medium were isotropic in resistivity under stress. An approximate correction has been worked out by H. Suhl of these laboratories and is

$$\Pi_T = \Pi_T(\text{obs}) + \frac{\omega}{2\pi l}(\Pi_T - \Pi_L), \quad (2)$$

where the  $\Pi$ 's are  $(1/X)\delta \rho/\rho$ ,  $L$  and  $T$  stand for longitudinal and transverse,  $\omega$  is the width of the specimen, and  $l$  the length of the transverse electrode. This correction is nearly negligible for the reported results for arrangement B. It amounts to around 10 percent for the reported values of arrangement D and its uncertainty becomes significant. Arrangement D, how-

<sup>11</sup> E. M. Conwell, Proc. Inst. Radio Engrs. 40, 1327 (1952).

TABLE I. Values of  $(1/X)(\delta\rho/\rho)$  in units of  $10^{-12}$  cm<sup>2</sup> dyne<sup>-1</sup> for the experimental arrangements shown in Fig. 1. The values of D calculated were obtained by combining observation A, B, and C. The observations are adiabatic. The specimen resistivities are in ohm-cm.

Type, material, and resistivity	Observed				Calculated
	A $\Pi_{11}$	B $\Pi_{12}$	C $\frac{1}{2}(\Pi_{11}+\Pi_{12}+\Pi_{44})$	D $\frac{1}{2}(\Pi_{11}+\Pi_{12}-\Pi_{44})$	D $\frac{1}{2}(\Pi_{11}+\Pi_{12}-\Pi_{44})$
<i>n</i> Ge 1.5	-2.3		-71.8		
<i>n</i> Ge 5.7	-2.7	-3.9	-71.7	+62.0	+65.1
<i>n</i> Ge 9.9	-4.7	-5.0	-73.8	+66.2	+64.1
<i>n</i> Ge 16.6	-5.2	-5.5	-74.7	+67.9	+64.0
<i>p</i> Ge 1.1	-3.7	+3.2	+48.1		
<i>p</i> Ge 15.0	-10.6	+5.0	+46.5		
<i>n</i> Si 11.7	-102.2		-31.2		
<i>n</i> Si 18.6	-102.2		-31.0		
<i>p</i> Si 7.8	+6.6	-1.1	+71.8		
<i>p</i> Si 22.7	+6.5		+71.9		

ever, has been used only as an internal check of the derived coefficients. The combined results omit this observation.

### Precision and Errors

By the nature of the apparatus the electrical precision was constant at something better than one percent in  $\delta V$  for all specimens except those where a combination of two out of three things obtained: low resistivity, transverse electrodes, or small piezoresistance.

The crystallographic orientations of the final rods were within 20 minutes of the nominal values in all cases. This accuracy of alignment is quite satisfactory because the piezoresistance effect, although highly anisotropic, varies as the square of the error angle at the orientations used.

The transverse measurements are generally of less precision than the longitudinal simply because  $V$  is small. Moreover, a rectifying contact on such specimens will give a spurious reading arising in the energy gap effect.<sup>12</sup> The procedure which has been adopted is to test all transverse specimens for rectification, keeping only those which showed linear  $V$ - $I$  curves. Thus, for example, the transverse scheme failed entirely for *n* Si, and the necessary third observation was obtained by an isothermal pressure measurement.

The longitudinal results for *n* Ge and some of those for *p* Ge were obtained with rods to which the potential electrodes were directly applied by rhodium plating. All the silicon and most of the *p* Ge measurements were obtained with "bridges" which are rods with integral semiconductor side arms. Contacts could be made to the side arms which are well outside the stress field, thus eliminating any question of stress induced electrode effects. In several cases rod specimens were checked against bridge specimens with excellent agreement.

Certain specimens showed slight piezoresistance nonlinearity in the initial mounting, but this nonlinearity

<sup>12</sup> Hall, Bardeen, and Pearson, Phys. Rev. 84, 129 (1951).

was removed in all cases by straightening the mount or remounting. Another indication that these small effects were caused by poor alignment of grips and sample was the inconsistency of the magnitude and sign of this nonlinearity. The origin of the nonlinearity has not been tracked down but there are several ways in which nonuniform or biaxial stress plus tensor piezoresistance could account for it.

### Conditions

The piezoresistance was observed with the specimen in a thermally lagged and reasonably light tight enclosure. The room temperature results were either obtained at  $25 \pm 1^\circ\text{C}$  or a short extrapolation was made to that temperature. The low-temperature results were obtained by mounting the specimen in a dewar flask over boiling liquid N<sub>2</sub>.

The resistivity values which have been studied were chosen to be below the point where minority carrier conduction is important and above the point where impurity scattering becomes significant.

The present observations are considered to be adiabatic rather than isothermal. The measured thermal time constant of the specimens in their measurement environment was about 15 seconds, while the time constant of the amplifier was 0.6 second. The difference between the isothermal and adiabatic values is small in any case, roughly  $0.5 \times 10^{-12}$  cm<sup>2</sup> dyne<sup>-1</sup>.

### RESULTS

Table I shows the end product of the foregoing procedures; the entries in that table are termed observations. The tensor nature of the piezoresistance effect is outlined in the appendix where it is shown how the observations A, B, and C may be expressed in terms of the elements  $\Pi_{11}$ ,  $\Pi_{12}$ , and  $\Pi_{44}$  of the pertinent fourth rank tensor. It is more interesting, however, to quote the results in the form of three other constants which are combinations of the actual tensor elements.

In the case of cubic crystals there are three combinations of the elastic constants  $C_{ij}$ , namely  $(C_{11}+2C_{12})/3$ ,  $C_{44}$  and  $(C_{11}-C_{12})/2$  which relate crystallographically simple stresses to the corresponding strains and which have been termed fundamental elastic constants. For germanium and silicon there are three similar combinations of piezoresistance coefficients  $\Pi_{11}+2\Pi_{12}$ ,  $\Pi_{44}$ , and  $\Pi_{11}-\Pi_{12}$ . The combination  $\Pi_{11}+2\Pi_{12}$  is the negative of the pressure coefficient. The shear coefficients  $\Pi_{44}$  and  $\Pi_{11}-\Pi_{12}$  give the transverse electric field which develops when an appropriate shear stress is applied, but it is simpler to consider their meaning directly in terms of hypothetical modifications of the present experiments C and A, respectively. The coefficient  $\Pi_{44}$  would give directly  $(1/X)(\delta\rho/\rho)$  in arrangement C if, in addition to the longitudinal tensile stress  $X$ , an equal transverse compression were also applied. The two stresses effectively change the angle between

two [100] type directions. The coefficient  $\Pi_{11}-\Pi_{12}$  bears the same relation to arrangement *A*, the stresses changing the angle between two orthogonal [110] directions. These constants are listed in Table II.

The shear constants  $\Pi_{44}$  and  $\Pi_{11}-\Pi_{12}$  have the same adiabatic and isothermal values. The adiabatic pressure coefficient is listed as directly determined from the observations. The isothermal pressure coefficients were obtained by applying the appropriate correction, using for the temperature coefficients of resistance the values given by conventional mobility-temperature laws except for the 16.6 ohm-cm *n* Ge sample where the negative temperature coefficient of resistance was measured. Values of the isothermal pressure coefficient determined by Bridgman for several samples of *n* and *p* Ge have been included in Table II for comparison. The latter have been corrected slightly for dimensional changes.

TABLE II. Values of the derived piezoresistance coefficients in units of  $10^{-12}$  cm<sup>2</sup> dyne<sup>-1</sup>. Resistivities are in ohm-cm.

Type, material, and resistivity	$\Pi_{44}$	$\Pi_{11}-\Pi_{12}$	$-\frac{1}{P} \frac{\delta\rho}{\rho} = \Pi_{11}+2\Pi_{12}$	
			Adiabatic	Isothermal
<i>n</i> Ge 1.5	-138.1	+ 1.0	(- 8.7) <sup>a</sup>	- 7.0
<i>n</i> Ge 4.2 <sup>b</sup>				- 8.3
<i>n</i> Ge 5.7	-136.8	+ 1.2	-10.5	- 8.8
<i>n</i> Ge 8.4 <sup>b</sup>				- 9.8
<i>n</i> Ge 9.9	-137.9	+ 0.3	-14.7	-13.0
<i>n</i> Ge 16.6	-138.7	+ 0.3	-16.2	-17.9
<i>n</i> Ge 18.5 <sup>b</sup>				-27.1
<i>p</i> Ge 0.9-3.3 <sup>c</sup>				+ 2.5
<i>p</i> Ge 1.1	+ 96.7	- 6.9	+ 2.7	+ 5.2
<i>p</i> Ge 15.0	+ 98.6	- 15.6	- 0.6	+ 1.9
<i>n</i> Si 11.7	- 13.6	-155.6	+ 4.6	+ 5.7 <sup>d</sup>
<i>p</i> Si 7.8	+138.1	+ 7.7	+ 4.4	+ 6.0

<sup>a</sup> This value extrapolated from *n* Ge 5.7 and *n* Ge 9.9.

<sup>b</sup> P. W. Bridgman (see reference 13) and by letter. Values are from the initial pressure effect.

<sup>c</sup> P. W. Bridgman (see reference 13). There were six specimens in this resistivity range, five of which were consistent at the value shown and one of which showed zero pressure effect.

<sup>d</sup> Measured directly.

The elastoresistance coefficients defined in the appendix relate the fractional resistivity change to the strain and have the advantage of putting all the coefficients for all the materials on a comparable strain basis. Simple combinations of these have meanings similar to those for the fundamental piezoresistance coefficients. In particular  $(m_{11}+2m_{12})/3 = d \ln\rho/d \ln v$  is the volume dilation coefficient. The shear constant  $m_{44}$  gives  $(1/e)(\delta\rho/\rho)$  in arrangement *C* when the longitudinal strain  $e/2$  and the transverse strain  $-e/2$  are imposed. The shear constant  $(m_{11}-m_{12})/2$  is similarly related to arrangement *A*. These fundamental elastoresistance coefficients are listed in Table III.

#### DISCUSSION OF THE RESULTS

The coefficients presented in Table II or in Table III are of both signs and show a wide range of magnitudes

reflecting the very high anisotropy of the piezoresistance in these cubic materials. A convenient measure of the anisotropy is the quantity  $\Pi_{44}/\frac{1}{2}(\Pi_{11}-\Pi_{12})$  (or its reciprocal for *n* Si); the smallest value of 14 here for this quantity contrasts with the frequent value of three for the equivalent elastic anisotropy. The fundamental constants separate the large and small effects, and the discussion below is divided up accordingly.

Tables II and III list essentially 12 coefficients (four materials  $\times$  3 types of constant). It may be noted initially that four of these vary with resistivity, *viz.*, the pressure effect for *n* germanium and all three coefficients for *p* germanium. The other eight constants are believed not to vary with resistivity within the experimental uncertainty. This conclusion must be reached for silicon by inspection of Table I, where the important longitudinal observations show such marked independence of resistivity that the difficult third observation was made only for the lower resistivity value. It is hardly conceivable that  $\Pi_{12}$  and  $\Pi_{44}$  should *both* vary in just such a way as to keep  $\frac{1}{2}(\Pi_{11}+\Pi_{12}+\Pi_{44})$  constant.

#### The Pressure Effect

Values of the isothermal  $\Pi_{11}+2\Pi_{12}$  in Table II are convenient to consider first because several values directly determined by Bridgman<sup>13</sup> for *n* germanium are available for comparison. Inspection of the combined total of seven measured values show that they vary smoothly with resistivity. Closer inspection shows that  $\Pi_{11}+2\Pi_{12}$  is linear with the resistivity squared and the resistivity variation is therefore assigned entirely to the energy gap effect as discussed in the introduction. The slope of the  $\rho^2$  plot is correct for this mechanism. The energy gap effect may then be extrapolated out allowing one to deduce a value of the pressure coefficient which describes the effect of pressure on *lattice* mobility alone without the complication of a change in charge carrier number.

For *p*-type germanium the sign of  $\Pi_{11}+2\Pi_{12}$  agrees with that determined by Bridgman at low resistivity, but the magnitude does not. No reason for this discrepancy has been discovered, our own measurements

TABLE III. Values of the dimensionless elastoresistance constants. Resistivities are in ohm-cm.

Type, material, and resistivity	$m_{44}$	$\frac{m_{11}-m_{12}}{2}$	$\frac{d \ln\rho}{d \ln v} = \frac{m_{11}+m_{12}}{3}$	
			Adiabatic	Isothermal
<i>n</i> Ge 1.5	- 93.0	+ 0.4	- 6.6	- 5.3
<i>n</i> Ge 5.7	- 92.0	+ 0.5	- 8.0	- 6.8
<i>n</i> Ge 9.9	- 92.8	+ 0.1	-11.1	- 9.8
<i>n</i> Ge 16.6	- 93.4	+ 0.1	-12.3	-13.6
<i>p</i> Ge 1.1	+ 65.1	- 2.8	+ 2.0	+ 3.9
<i>p</i> Ge 15.0	+ 66.5	- 6.3	- 0.5	+ 1.4
<i>n</i> Si 11.7	- 10.8	-79.5	+ 4.6	+ 5.7
<i>p</i> Si 7.8	+110.0	+ 3.9	+ 4.4	+ 6.0

<sup>13</sup> P. W. Bridgman, Proc. Am. Acad. Arts Sci. 82, 71 (1953).

having been repeated with other specimens as were Bridgman's. In any case upon intercomparing the present low- and high-resistivity pressure coefficients the effect of the energy gap is again apparent, the change in coefficient being, correctly, in the same direction as for  $n$ -type germanium. The magnitude of the resistivity dependence is also very roughly correct, but the point need not be belabored when only two data are available. The fact that the pressure effect in both types of silicon is apparently independent of resistivity (again see Table I) would seem to imply zero energy gap effect at room temperature and at these resistivities.

The values of  $(m_{11}+2m_{12})/3 = d \ln \rho / d \ln v$  for silicon and at the lowest resistivity in germanium then describe the effect of a volume change on the mobility. Such values may be compared in sign and magnitude with those given by Eq. (1) which basically describes the effect of volume dilation on the amplitude of the thermal waves and hence on mobility. The values shown in Table II have the normal positive sign given by Eq. (1) except for  $n$  germanium which is anomalous. The same quantity for Li, Ca, and Sr has anomalous sign. Frank has suggested that the negative sign in Li

results from a decrease with volume of the effective mass of the electrons.<sup>9</sup>

The assumptions underlying Eq. (1) are valid only at temperatures above the characteristic temperature. This condition is not met by silicon and only barely by germanium so that magnitudes may be compared only as to order. For  $p$  germanium the experimental value of  $(m_{11}+2m_{12})/3$  is somewhere between two and five compared with the calculated value of 1.7. Both types of silicon give about 4.5 compared with the calculated 1.4. Thus Eq. (1) gives at least the right order of magnitude for these three coefficients.

### The Small Shear Coefficient

For each of the materials studied one of the shear constants is large and one is small. The small ones are  $(m_{11}-m_{12})/2$  for  $n$  Ge (zero within the experimental uncertainty),  $p$  Ge (-2.8 to -6.3) and  $p$  Si (+3.9). The coefficient  $m_{44}$  is small for  $n$  Si (-10.8). The resistivity dependence of  $(m_{11}-m_{12})/2$  for  $p$  Ge is certainly real. These values for the small shear coefficient are also of the order of magnitude of what one would expect from the shear analog of Eq. (1). It thus seems unprofitable to look for a more detailed mechanism than that of the effect of strain in general on the thermal wave amplitude in the case of three volume dilation coefficients and all four of the smaller shear coefficients.

### The Large Shear Coefficient

The shear coefficient  $m_{44}$  is large for  $n$  Ge (-93),  $p$  Ge ( $\sim +66$ ), and  $p$  Si (+110). The coefficient  $(m_{11}-m_{12})/2$  is, on the other hand, the large one for  $n$  Si (-80). The variation with resistivity of  $m_{44}$  in the case of  $p$  Ge is small but is nevertheless felt to be real. The fact that the sign of the large effect is the same as that of the charge carriers is at worst useful as a mnemonic.

The large shear coefficients are at least one order of magnitude larger than one would expect from the effect of strain on the amplitude of the thermal waves. It is evident that an explanation of these large coefficients must be sought in an essentially different mechanism. One such new mechanism which can account for large shear coefficients is described below.

### ELECTRON TRANSFER MECHANISM

C. Herring of these laboratories has suggested such an effect based on current theoretical ideas of the structure of the energy bands in these materials.<sup>14</sup> The suggested effect is quite capable of producing a large shear coefficient and automatically predicts the high anisotropy which the experiment shows. The mechanism in the form which will be outlined applies particularly to  $n$  Si and  $p$  Ge. We state in advance that there is

<sup>14</sup> F. Herman, Phys. Rev. **88**, 1210 (1952); F. Herman and J. Callaway, Phys. Rev. **89**, 518 (1953).

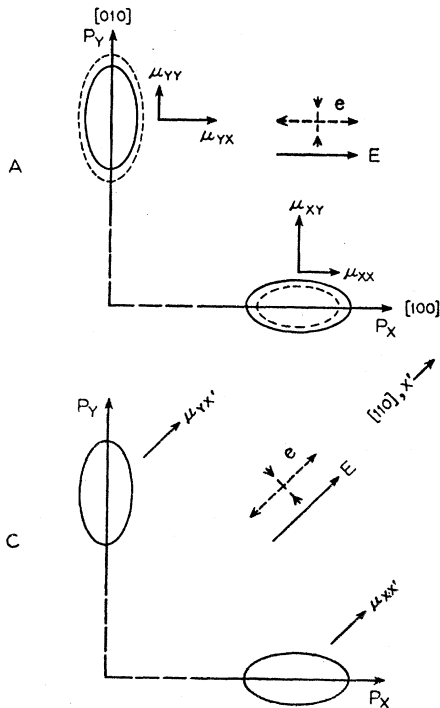


FIG. 2. Schematic diagram of probable constant energy surfaces in momentum space for  $n$  Si. The electrons are located in six energy valleys at the centers of the constant energy ellipses which are shown greatly enlarged. The effect of stress on the two valley energies shown is indicated by the dotted ellipsoids. The mobilities of the several groups of charge carriers in various directions are roughly indicated by the arrows. The diagrams correspond to the two experimental arrangements A and C of Fig. 1.

agreement with theory for  $n$  Si but disagreement for  $p$  Ge.

The structure of the constant energy surfaces in  $n$  Si is at present thought to be as indicated in Fig. 2. These surfaces consist of ellipsoids of revolution located on the cube axes in momentum space, the six-ellipsoid picture.<sup>15</sup> The electrons are located in the energy minima which means that there are six groups of them centered at the ellipsoid centers. Because the surfaces are ellipsoidal the effective mass of an electron in a given group is anisotropic. Hence, the mobility associated with a group is anisotropic although the overall mobility is not. The energy value at a minimum will furthermore be sensitive to a normal strain component in the direction of the minimum.

Figure 2 corresponds to experimental arrangement  $A$  except that the simple strain system defining  $(m_{11}-m_{12})/2$  is indicated rather than the tensile stress  $X$ . The electric field and the current are in the  $[100]$  direction. In the absence of strain the two energy valleys shown are equally populated with electrons, but the two groups of electrons have different mobilities in the  $[100]$  direction. When the strain system is applied, the two energy minima shift in opposite directions indicated by the shift of a given constant energy surface from the full to the dashed positions. There are then two effects of roughly comparable importance: (a) the electrons transfer from the  $x$  valley to the lower-energy  $y$  valley, and (b) the probability of an electron being scattered from a  $y$  valley into an  $x$  valley is decreased. In the strained state there are then more electrons that have high mobility and fewer electrons of low mobility in the field direction. Hence  $\delta\rho/\rho$  and  $(m_{11}-m_{12})/2$  are negative and finite for the situation assumed in Fig. 2. The experimental value for this constant in  $n$  Si is negative and large.

The sign of the electron transfer effect is changed by (a) making the ellipsoids oblate rather than prolate or (b) by reversing the direction of the energy shift. The present measurements eliminate two of the four possible combinations but cannot distinguish between the remaining two. Figure 2 has merely been drawn to be consistent with the experimental result for  $n$  Si. The order of magnitude of the effect is determined by the ellipsoid axial ratio and by a factor  $\Delta E/kT$ , where  $\Delta E$  is the energy shift per unit strain. The experimental result of  $-80$  for  $(m_{11}-m_{12})/2$  for  $n$  Si requires  $\Delta E$  to be of the order of several electron volts, which is reasonable.

The electron transfer mechanism furthermore predicts a zero contribution to the  $m_{44}$  coefficient for the six ellipsoid picture. This fact is shown by Fig. 2 which corresponds with experimental arrangement  $C$  except again for the strain. The mobilities of the  $x$  and  $y$  groups of electrons are the same in the  $[110]$  direction and the strain shifts the energy of the two valleys the

same, i.e., not at all. In both essential respects the mechanism will give zero effect. This is reflected in the low value of  $m_{44}$  for  $n$  Si.

In using Fig. 2 the ellipsoids in the  $z$  direction have been ignored. The *strain* systems considered do not affect these energy valleys and so for small strains their electron population will not be changed. This statement does not hold for the *stress* system imposed in arrangement  $C$ , Fig. 1. The moderately high value of observation  $C$  for  $n$  Si reflects the presence of the  $z$  ellipsoids.

The same argument can be carried through for other arrangements of ellipsoids consistent with cubic symmetry although such arrangements are not suggested by the energy band calculations. In particular, arrangements of eight  $[111]$  ellipsoids and 12  $[110]$  ellipsoids have been considered. The eight  $[111]$  ellipsoid picture predicts a definite  $m_{44}$  contribution and a zero  $(m_{11}-m_{12})/2$  contribution roughly corresponding to the experimental results for  $n$  and  $p$  Ge and  $p$  Si. The 12  $[110]$  ellipsoid picture predicts that both shear constants will be finite, of the same sign, and that  $m_{44} > (m_{11}-m_{12})/2$ . The predicted  $[110]$  electron transfer anisotropy is not large, however, in disagreement with all the present results.

The situation relating the electron transfer mechanism plus ellipsoid picture to the present piezoresistance results may be summarized simply. *If ellipsoids are present and if the electron transfer mechanism is the principal one operating, then the ellipsoids must be located on  $[100]$  axes for  $n$  Si and on  $[111]$  axes for the other three types of material.*

In the case of  $p$  germanium the above qualified conclusion of  $[111]$  ellipsoids does not agree with the energy band calculations which suggest that  $[111]$  ellipsoids are unlikely. There are, also, several other types of experiment which will not be discussed but which favor the six  $[100]$  ellipsoid picture for  $p$  germanium. The existence of another or an additional mechanism must be considered seriously therefore. The strain may produce a change of resistance through its action on the phonons, on the electrons, and on the coupling between them. As has been pointed out above, the strain-phonon effect can account for small piezoresistance coefficients. The electron transfer effect is one possible action of strain on the electrons. The possibility of another strain-electron or of a strain-coupling action remains for  $p$  germanium.

There are indeed two indications in the present experiments that  $p$  germanium is different from the other materials. The shear constants show a definite resistivity dependence in contrast to the other materials, and the temperature dependence of the piezoresistance in  $p$  Ge is different from the others. Preliminary measurement of the temperature dependence of the large shear coefficient has been carried out from 300 to 200°K. For this purpose only the specimen  $A$  or  $C$  giving the large observation was used. The temperature

<sup>15</sup> W. Shockley, Phys. Rev. **90**, 491 (1953).

curves were fitted to the equation  $\Pi = AT^{-b}$  at 300 and 200°K. The values of  $b$  are 0.8 for  $n$  Ge, 1.1 for  $p$  Ge, 0.7 for  $n$  Si, and 0.6 for  $p$  Si. These two facts suggest that an additional mechanism is operating in  $p$  germanium.

The discussion of the electron transfer mechanism has been made in terms of ellipsoidal constant energy surfaces for the sake of definiteness. It should be pointed out that all that is really required for the mechanism is that the energy surfaces be nonspherical at the location of the charge carriers. The ellipsoid picture is not particularly indicated by the energy band calculations for  $n$  Ge and  $p$  Si but, other nonspherical energy surfaces could equally well produce the electron transfer effect and consequently highly anisotropic piezoresistance. The present results would then show, again assuming the electron transfer mechanism, that the charge carriers are located principally in  $[111]$  directions in momentum space for  $n$  germanium and  $p$  silicon.

#### ACKNOWLEDGMENT

The author is grateful for the opportunity of spending a year at Bell Telephone Laboratories on leave of absence from Case Institute of Technology. In this work he has had help and advice from his colleagues J. A. Hornbeck, J. R. Haynes, G. L. Pearson, W. L. Bond, T. S. Benedict, W. P. Mason, and W. Shockley in addition to those named in the text. He is indebted to W. Augustyniak for excellent technical assistance.

#### APPENDIX

##### Cubic Piezoresistance Coefficients

The change of resistivity is a symmetrical second rank tensor as is the stress. The tensor connecting the two is therefore of fourth rank, and the piezoresistance effect is strictly analogous to the piezooptical effect<sup>4</sup> with the resistivity replacing the dielectric constant. For germanium and silicon three coefficients are required to specify completely the piezoresistance property. In this section we make the necessary definitions and show how the fundamental piezoresistance and elastoresistance coefficients of the text may be computed from the observations. The restriction of a cubic crystal is imposed immediately on the resistivity. Crystal symmetry conditions are used later to restrict the conclusion of three piezoresistance constants to the cubic crystal classes  $T_d$ ,  $O$ , and  $O_h$ , four constants being required for the other two cubic classes  $T$  and  $T_h$ . For convenience the same matrix notation as has been used relatively recently for the piezooptical effect<sup>16</sup> will be used here.

The starting point of the analysis is

$$E = \rho J, \quad (3)$$

where  $E$  is the electric field,  $J$  the current density and

<sup>16</sup> W. L. Bond, Bell System Tech. J. 22, 1 (1943).

$\rho$  a three by three symmetrical matrix<sup>17</sup> in the general case of a triclinic crystal and arbitrary reference axes. For a cubic crystal and arbitrary axes the  $\rho$  matrix reduces to a scalar, but it is convenient here to continue thinking of it as a matrix. If a change in  $\rho$  occurs because of stress, one may write for the *special case of constant current density*, which applies in the present experiments,

$$\delta E = (\delta \rho) J; \quad (4)$$

$\delta E$  is now the change in electric field, a vector, and  $(\delta \rho)$  is again a three-by-three symmetrical matrix. For a cubic crystal it is convenient to divide through by the scalar resistivity, giving

$$\delta E = \Delta J, \quad (5)$$

and then to write out explicitly:

$$\begin{aligned} \delta E_1/\rho &= \Delta_{11}J_1 + \Delta_{12}J_2 + \Delta_{13}J_3, \\ \delta E_2/\rho &= \Delta_{12}J_1 + \Delta_{22}J_2 + \Delta_{23}J_3, \\ \delta E_3/\rho &= \Delta_{13}J_1 + \Delta_{23}J_2 + \Delta_{33}J_3, \end{aligned} \quad (6)$$

where  $\Delta_{ij} = (\delta \rho)_{ij}/\rho$ . The nondiagonal terms are not necessarily zero, nor are the diagonal terms equal in a general frame of reference in a cubic crystal. The quantity  $\Delta$  relating a vector  $\delta E$  to a vector  $J$  transforms just like the stress or the dielectric constant but not like the conventional strain. The diagonal terms in  $\Delta$  giving the change in field along the corresponding current density component are in a crude sense analogous to an elastic normal strain; the nondiagonal terms give the change in field (the field which develops in the cubic case) normal to a given current density component, and may be thought of as electrical shear strains.

The matrix  $\Delta$  may be written as a six element column matrix using the descending sequence  $\Delta_{11}$ ,  $\Delta_{22}$ ,  $\Delta_{33}$ ,  $\Delta_{23}$ ,  $\Delta_{31}$ ,  $\Delta_{12}$ , and the stress  $X$  may be similarly written. The connection between  $\Delta$  and  $X$  may be written for a cubic crystal using *general reference axes* as

$$\Delta = \Pi X, \quad (7)$$

where  $\Pi$  is a six-by-six matrix of piezoresistance constants. This matrix is not quite symmetrical even for the cubic case and not at all symmetrical for a triclinic crystal in the generalized version of Eq. (7). If now the cubic axes  $[100]$ ,  $[010]$ , and  $[001]$  are chosen as reference axes and the symmetry of any one of the cubic crystal classes  $T_d$ ,  $O$ , or  $O_h$  is used it can be shown that  $\Pi$  reduces to

$$\Pi = \begin{pmatrix} \Pi_{11} & \Pi_{12} & \Pi_{12} & 0 & 0 & 0 \\ \Pi_{12} & \Pi_{11} & \Pi_{12} & 0 & 0 & 0 \\ \Pi_{12} & \Pi_{12} & \Pi_{11} & 0 & 0 & 0 \\ 0 & 0 & 0 & \Pi_{44} & 0 & 0 \\ 0 & 0 & 0 & 0 & \Pi_{44} & 0 \\ 0 & 0 & 0 & 0 & 0 & \Pi_{44} \end{pmatrix}. \quad (8)$$

Germanium and silicon belong to crystal class  $O_h$ .

<sup>17</sup> For a good discussion see W. Boas and J. K. MacKenzie in *Progress in Metal Physics* (Interscience Publishers, Inc., New York, 1950), Vol. 2, p. 93.

Experimental arrangements *A* and *B* make use of just this array of coefficients. In both arrangements  $X_{11}=X$  and all other stresses are zero. The electrode arrangement of *A* measures  $\Delta_{11}$  and that of *B* measures  $\Delta_{22}$ ; thus for *A*,  $\Pi_{11}=\Delta_{11}/X_{11}$ , and for *B*,  $\Pi_{12}=\Delta_{22}/X_{11}$  are directly measured.

The choice of axes in arrangements *C* and *D* permits  $\Pi_{44}$  to be determined in a simple but indirect way. For the reference axes  $[110]$ ,  $[\bar{1}10]$ ,  $[001]$  the transformation of Eq. (8) gives for arrangement *C*,  $\frac{1}{2}(\Pi_{11}+\Pi_{12}+\Pi_{44})=\Delta_{11}/X_{11}$  and for *D*,  $\frac{1}{2}(\Pi_{11}+\Pi_{12}-\Pi_{44})=\Delta_{22}/X_{11}$ . Thus all three piezoresistance coefficients can be determined using *A*, *B*, and *C*, with *D* left over as a check on internal consistency. Table I shows that the agreement between the observed *D* and the value calculated from *A*, *B*, *C* is reasonable in view of the approximate correction applied to *D*.

The necessary third observation cannot be obtained by making another longitudinal measurement in a third crystallographic direction. The general longitudinal effect is given by  $\Pi_{11}'=\Pi_{11}-2\Pi\Gamma$ , where  $\Pi=\Pi_{11}-\Pi_{12}-\Pi_{44}$  and  $\Gamma$  is an orientation function. Only  $\Pi_{11}$  and the combination  $\Pi$  can be determined by longitudinal measurements alone, and thus the third measurement must be of a different type. The transverse observation *B* serves this purpose.

The equations reducing the observations to the fundamental piezoresistance coefficients defined in the

text are then,

$$\begin{aligned}\Pi_{11}+2\Pi_{12}&=A+2B, \\ \Pi_{44}&=2C-A-B, \\ \Pi_{11}-\Pi_{12}&=A-B,\end{aligned}\quad (9)$$

where *A*, *B*, and *C* refer to the numbers given in Table I.

A set of elastoresistance coefficients also can be deduced from the present results. The change-in-resistivity matrix  $\Delta$  can be related to the strain *e* by the elastoresistance coefficients *m*,

$$\Delta=me, \quad (10)$$

where the strain *e* is, to be explicit, the six-element column matrix of terms  $\partial u/\partial x$ ,  $\partial v/\partial y$ ,  $\partial w/\partial z$ ,  $[(\partial v/\partial z)+(\partial w/\partial y)]$ ,  $[(\partial w/\partial x)+(\partial u/\partial z)]$ ,  $[(\partial u/\partial y)+(\partial v/\partial x)]$ , where *u*, *v*, *w* are the displacements of a point with coordinates *x*, *y*, *z*. Since we have for the relation between stress and strain,

$$X=Ce, \quad (11)$$

where *C* is the elastic constant matrix, it follows, using Eq. (7) that

$$m=IC. \quad (12)$$

The fundamental strain coefficients are quickly given by the aid of this last relation and a little algebra as

$$\begin{aligned}\frac{1}{3}(m_{11}+2m_{12})&=(\Pi_{11}+2\Pi_{12})(C_{11}+2C_{12})/3, \\ m_{44}&=\Pi_{44}C_{44}, \\ \frac{1}{2}(m_{11}-m_{12})&=(\Pi_{11}-\Pi_{12})(C_{11}-C_{12})/2.\end{aligned}\quad (13)$$